Brief Communications

Dynamic Regulation of Synaptic Maturation State by Voltage-Gated A-Type K^+ Channels in CA1 Hippocampal Pyramidal Neurons

Eunyoung Kim and Dax A. Hoffman

Molecular Neurophysiology and Biophysics Unit, Program in Development Neuroscience, Eunice Kennedy Shriver National Institute of Child Health and Human Development, National Institutes of Health, Bethesda, Maryland 20892

Neuronal activity is critical for the formation and modification of neural circuits during brain development. In hippocampal CA1 pyramidal dendrites, A-type voltage-gated K^+ currents, formed primarily by Kv4.2 subunits, control excitability. Here we used Kv4.2 knock-out (Kv4.2-KO) mice along with acute *in vivo* expression of Kv4.2 or its dominant-negative pore mutant to examine the role of Kv4.2 in the development of CA1 synapses. We found that Kv4.2 expression induces synaptic maturation in juvenile WT mice and rescues developmentally delayed synapses in adult Kv4.2-KO mice. In addition, we show that NMDAR subunit composition can be reverted back to the juvenile form in WT adult synapses by functionally downregulating Kv4.2 levels. These results suggest that Kv4.2 regulation of excitability determines synaptic maturation state, which can be bidirectionally adjusted into adulthood.

Introduction

Neuronal activity is thought to play a critical role in the formation and modification of neural circuits during brain development while the disruption of normal neuronal activity and synaptic plasticity has been implicated in several neurological disorders (Lynch, 2004). While the molecular mechanisms underlying activity-dependent synaptic modification during development are not fully understood, at excitatory synapses in the CNS, NMDA-type glutamate neurotransmitter receptors (NMDARs) have been shown to play important roles in brain development in addition to synaptic plasticity and cognitive functions (Bliss and Collingridge, 1993; Malenka and Nicoll, 1999; Lynch, 2004). A current theory for the pathophysiology of schizophrenia implicates hypofunction of NMDA receptor signaling (Gaspar et al., 2012), and dysfunction of the glutamatergic system has been implicated in other psychiatric disorders such as Alzheimer's disease, ADHD, and depression (Wallace et al., 2011).

Early in development, excitatory synapses in the hippocampus transmit primarily through NMDARs (Kerchner and Nicoll, 2008). These synapses are functionally silent early in development, becoming functional with experience-dependent insertion of AMPA-type glutamate receptors (AMPARs) (Kerchner and Nicoll, 2008). In addition, as synapses mature, those containing GluN2A NMDAR subunits replace GluN2B-containing NMDARs (Sans et al., 2000). These synaptic modifications require precise control of neuronal activity but the molecular mechanisms underlying them are not fully understood. A-type K^+ currents play an important role for neuronal excitability and synaptic plasticity (Birnbaum et al., 2004). A-type K^+ channels activate at subthreshold membrane potentials, inactivate rapidly, and quickly recover from inactivation. A-type K^+ channels regulate the threshold for action potential (AP) initiation, repolarization, frequency-dependent AP broadening, and control the back-propagation of action potentials and LTP induction (J. Kim et al., 2005; Chen et al., 2006; Nerbonne et al., 2008). Among the several different types of K^+ channel pore-forming subunits that produce A-type K^+ currents (e.g., Kv1, Kv3, and Kv4) that have been identified, Kv4.2 is the most prominent in hippocampal CA1 pyramidal neurons (J. Kim et al., 2005; Chen et al., 2006; Lauver et al., 2006). Recent studies have found that elimination of Kv4.2 lowered the threshold for LTP induction and increased the threshold of LTD (Chen et al., 2006; Zhao et al., 2011). Conversely, increased Kv4.2 expression was found to prevent LTP induction (Jung et al., 2008). Moreover, increased expression of Kv4.2 in organotypic slices caused a decrease in synaptic GluN2B/GluN2A ratio, whereas downregulation of Kv4.2 resulted in an increased proportion of synaptic GluN2B/GluN2A (Jung et al., 2008). These results suggest a possible role for Kv4.2 in regulating NMDAR subunit composition during development. Therefore, we examined the role of Kv4.2 in synaptic development and maturation by manipulating functional Kv4.2 expression *in vivo* via injection of virus containing either eGFP-labeled Kv4.2 (Kv4.2g) or a dominant-negative pore mutation of Kv4.2 ($Kv4.2g^{W362F}$) into the hippocampal CA1 area in different aged groups of animals. Here we show

Received May 16, 2012; revised July 31, 2012; accepted Aug. 22, 2012.

Author contributions: E.K. and D.A.H. designed research; E.K. performed research; E.K. and D.A.H. analyzed data; E.K. and D.A.H. wrote the paper.

This work was supported by the National Institute of Child Health and Human Development Intramural Research Program. We thank Drs. Katherine Roche (NINDS) and Wei Li (NEI) for their critical review of earlier versions of this manuscript. We thank Begum Choudhury, Lin Lin, and Michael (Martin) Hatch for technical and experimental assistance.

Correspondence should be addressed to Dax A. Hoffman, 35 Lincoln Drive, MSC 3715, Building 35, Room 3C-905, Bethesda, MD 20892-3715. E-mail: hoffmand@mail.nih.gov.

DOI:10.1523/JNEUROSCI.2373-12.2012

 0270-6474/12/3214427-06$15.00/0

that Kv4.2 expression induced synaptic maturation in juvenile WT mice and rescued developmentally delayed synapses in adult Kv4.2 knock-out (Kv4.2-KO) mice. Moreover, NMDAR subunit composition reverted back to the juvenile form in adult WT synapses after functionally downregulating Kv4.2.

Materials and Methods

In vivo *viral infection and slice preparation.* Male C57BL/6J WT or Kv4.2-KO mice, aged P10–P12 or 8 weeks old, were injected with Sindbis virus containing either eGFP-tagged Kv4.2 (Kv4.2g) or Kv4.2g^{W362F} (J. Kim et al., 2005). Mice were anesthetized with ketamine/xylazine mixture (3.33 ml/kg) and then mounted in a stereotaxic instrument (David Kopf Instruments). Using a microsyringe pump controller (World Precision Instruments), 0.5–1 μl of virus was delivered into each hemisphere, targeting hippocampal area CA1. After the surgery, mice recovered from anesthesia and then were returned to their home cage. One or two days after injection, acute hippocampal slices (250 μm thick) were prepared in a cutting solution containing the following (in mM): 125 NaCl, 2.5 KCl, 25 $NaHCO_3$, 1.25 NaH_2PO_4, 25 glucose, 0.5 $CaCl_2$, 5 $MgCl_2$, pH 7.2. After 30 min incubation in normal ACSF (bubbled with 95% O_2, 5% CO_2) at 37°C, slices were transferred to room-temperature oxygenated ACSF solution. The National Institute of Child Health and Human Development's Animal Care and Use Committee approved all animal protocols.

Electrophysiology. Whole-cell recordings were obtained from infected or noninfected neurons under visual guidance using epifluorescence and transmitted light illumination. For patch-clamp recordings from acute hippocampal slices, slices were transferred to a submerged recording chamber with continuous flow of ACSF containing the following (in mM): 125 NaCl, 2.5 KCl, 25 $NaHCO_3$, 1.25 NaH_2PO_4, 25 glucose, 2 $CaCl_2$, 1 $MgCl_2$. Gabazine (10 μM) was added in all recordings. Patch electrodes (4–6 MΩ) were filled with the following (in mM): 100 Cs-gluconate, 0.6 EGTA, 5 $MgCl_2$, 8 NaCl, 2 Na_2ATP, 0.3 NaGTP, 40 HEPES, 15 CsCl, 1 QX-314, pH 7.25–7.3 by CsOH. To record whole-cell A-type currents, 1 μM TTX was added to the external solution and the internal solutions contained the following (in mM): 20 KCL, 125 Kglu, 10 HEPES, 4 NaCl, 0.5 EGTA, 4 ATP, 0.3 TriGTP, 10 Phosphocreatin, pH 7.2 by KOH.

EPSCs were induced by stimulation of the Schaffer-collateral pathway via monopolar electrodes located 100–200 μm from the recorded cell soma. The test stimulation in all EPSC experiments was set at 0.1 Hz and 0.2 ms duration and its intensity (100–900 μA) was adjusted to induce ~100 pA EPSCs at a holding potential of −60 mV. AMPAR-mediated EPSC amplitude was measured from an averaged trace of at least 10 sweeps. Amplitude and current charge of total and NMDAR-isolated EPSCs recorded at +40 mV were measured in traces averaged from 30 sweeps. After recording total EPSC amplitude at a +40 mV holding potential, 6,7-dinitroquinoxaline-2,3-dione (DNQX, 10 μM) was added to external recording solution to block AMPARs. NMDAR-mediated EPSCs were recorded after confirming the effect of DNQX by observing the complete blockade of AMPAR-mediated EPSCs recorded at −60 mV (5 min after application). Putative GluN2A-mediated EPSCs were then acquired by adding ifenprodil (3 μM) to external solution including DNQX. GluN2A-mediated EPSCs were recorded for 15 min after washing in DNQX+ifenprodil and the last 30 sweeps averaged.

Minimal stimulation experiments were performed at −60 mV and +40 mV holding potentials. Stimulation intensity was adjusted to the point that failure versus response could be clearly distinguished visually at −60 mV holding potential and then kept constant for the duration of the experiment.

Whole-cell recording parameters were monitored throughout each experiment and recordings where series resistances (15–20 MΩ) varied by >10% were rejected. All were performed at 31–32°C using a Multiclamp 700B amplifier with signals filtered at 1 kHz and digitized at 10 kHz via an Axon Digidata 1322A. Recordings were analyzed using Clampfit 10.1 (Molecular Devices), Microsoft Excel, Minianalysis (Synaptosoft), and IGOR Pro (WaveMetrics). Statistical tests performed were unpaired *t* test using Microsoft Excel or IGOR Pro. Significance was set to $p < 0.05$.

Immunoblotting. Whole hippocampi from P2, P10, 4-week-old, and 8-week-old WT or Kv4.2-KO mice were homogenized in a buffer solution containing the following (in mM): 50 TrisCl, 150 Nacl, 10 EGTA, 10 EDTA, 1% NP-40, and protease inhibitor mixture tablet (Roche). Protein concentrations were measured using a BCA kit (Pierce). Equal amounts of protein were separated by electrophoresis on 10% SDS bis-tris gels (Invitrogen) and transferred to nitrocellulose membranes. Immunoblotting was performed as previously described (J. Kim et al., 2005). Antibodies used were anti-Kv4.2 (1:1000; NeuroMab), anti-GluN2B (1:2000; BD Biosciences), anti-GluN2A (1:2000; Millipore), and β-actin (1:5000; Sigma). Quantification was performed using Odyssey software (LI-COR Bioscience). The values of total Kv4.2 protein were normalized to that of total β-actin used as a homogenate control from the same blots. To determine NMDAR subunit ratios, GluN2B and GluN2A were directly compared then normalized to the WT value from the same blot.

Results

To examine the impact of Kv4.2 expression on synaptic maturation, we characterized synaptic currents in WT and Kv4.2-KO mice at two different stages of development. In the hippocampus, NMDARs contain mostly GluN2A and GluN2B subunits, with the GluN2B/GluN2A ratio decreasing during development (Sans et al., 2000). We found that Kv4.2 protein expression in the hippocampus of WT mice also increased during development (relative to 8 weeks in WT; P2, 0.34 ± 0.04; P10, 0.73 ± 0.04; 4 weeks, 0.96 ± 0.2; $n = 3$). To measure the relative contribution of synaptic GluN2A and GluN2B subunits during development in WT and Kv4.2-KO mice, we pharmacologically isolated each component from total NMDAR-mediated EPSCs by bath applying the GluN2B antagonist ifenprodil (3 μM; Fig. 1*A*). In WT, the ifenprodil-sensitive fraction (ISF) was significantly decreased in adult hippocampal neurons compared with neonatal hippocampal neurons (neonatal, 0.49 ± 0.03, $n = 10$; adult, 0.11 ± 0.03, $n = 9$; $p < 0.01$; Fig. 1*B*), confirming a developmental decrease of synaptic GluN2B/2A ratio. However, there was no significant difference in ISF between neonatal and adult Kv4.2-KO mice (neonatal, 0.50 ± 0.04, $n = 5$; adult, 0.35 ± 0.05, $n = 10$; $p > 0.05$; Fig. 1*B*), indicating an enhancement of the fraction of total NMDAR current in adult Kv4.2-KO mice generated from GluN2B-containing NMDARs. Immunoblot analysis showed increased GluN2B/2A protein expression ratio in the hippocampus of Kv4.2-KO mice compared with that of WT mice throughout development (P10, 1.69 ± 0.3 of WT, $n = 5$; 8 weeks, 1.22 ± 0.05 of WT; $n = 5$). These results suggest that the normal developmental decrease of synaptic GluN2B was impaired or delayed in Kv4.2-KO mice.

Our results in Figure 1*B* suggest that developmental NMDAR subunit changes may require Kv4.2 activity. To determine if A-type K^+ currents drive synaptic maturation of developing synapses, we injected Kv4.2g into neonatal WT hippocampus (Fig. 1*C*). We first confirmed that Kv4.2g expression increased A-current amplitude in whole-cell recordings from neonatal WT mice 1 d after infection (Kv4.2g A-type current density, 215.93 ± 27.34 pA/pF, $n = 5$; uninfected, 127.20 ± 6.99, $n = 7$; $p < 0.01$). One day after expression of Kv4.2g, whole-cell recordings from neonatal WT CA1 neurons in acute slices showed decreased synaptic ISF (neonatal WT+Kv4.2g, 0.23 ± 0.03, $n = 11$; Fig. 1*D*,*E*) compared with uninfected neurons (neonatal WT, 0.49 ± 0.03, $n = 10$; $p < 0.01$).

The developmental conversion from primarily GluN2B-containing to GluN2A-containing NMDARs is regulated by experience (Yashiro and Philpot, 2008) and synaptic activity (Bellone and Nicoll, 2007). However, the activity-dependent

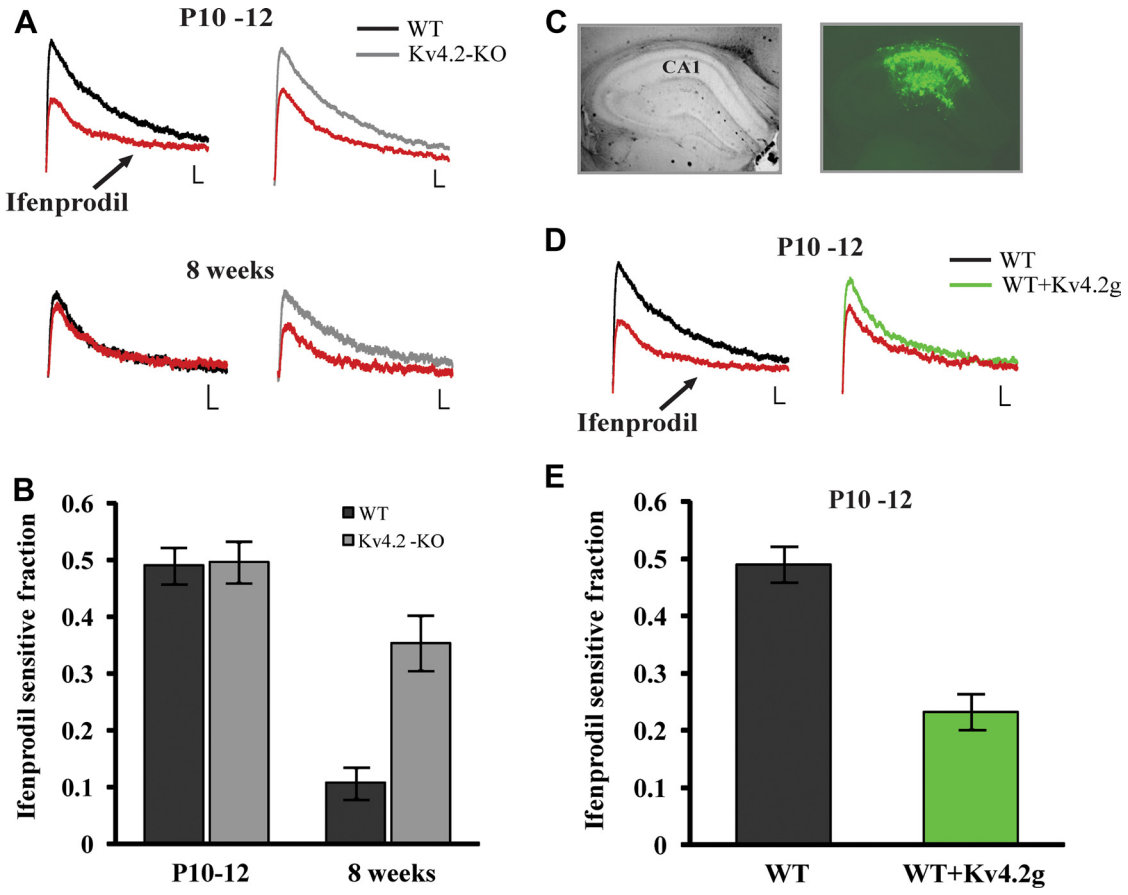

Figure 1. Increased GluN2B subunit composition in adult Kv4.2-KO mice. ***A***, Example traces of isolated NMDAR EPSCs recorded at +40 mV before and after ifenprodil (red trace) for pharmacological isolation of GluN2B subunit from WT (black trace) and Kv4.2-KO (gray trace) mice. Scale bars: 10 pA, 20 ms. ***B***, Averaged ifenprodil-sensitive fraction calculated from total NMDAR current charge (amplitude × ms). Error bars represent SEM. ***C***, Representative acute hippocampal slices prepared from WT mice injected *in vivo* with GFP Sindbis virus. Left, Differential interference contrast images; right, GFP fluorescence. ***D***, Example traces of NMDAR EPSCs before and after ifenprodil (red trace) from uninfected (black trace) and Kv4.2g-infected (green trace) neurons of neonatal WT mice. Scale bars: 10 pA, 20 ms. ***E***, Averaged ifenprodil-sensitive fractions from uninfected and infected neonatal WT neurons. Error bars represent SEM.

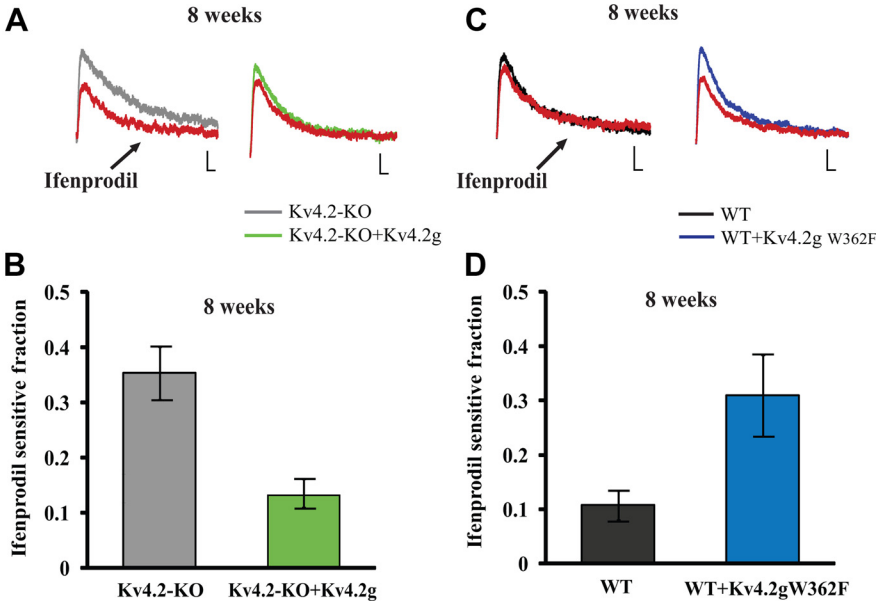

Figure 2. Kv4.2 bidirectionally regulates NMDAR subunit composition in adult hippocampal neurons. ***A***, Example traces of NMDAR EPSCs before and after ifenprodil (red trace) from uninfected (gray trace) and Kv4.2g-infected (green trace) neurons from adult Kv4.2-KO mice. Scale bars: 10 pA, 20 ms. ***B***, Averaged ifenprodil-sensitive fractions from uninfected and infected neurons from adult Kv4.2-KO mice. Error bars represent SEM. ***C***, Example traces of NMDAR EPSCs before and after ifenprodil (red trace) from uninfected (black trace) and Kv4.2g ^{W362F}-infected (blue trace) neurons from adult WT mice. Scale bars: 10 pA, 20 ms. ***D***, Averaged ifenprodil-sensitive fractions from uninfected and infected neurons from adult WT mice. Error bars represent SEM.

GluN2A-for-GluN2B NMDAR subunit switch in the hippocampus occurs only in neonatal, not mature, synapses (Bellone and Nicoll, 2007). We repeated the above experiments with adult Kv4.2-KO mice to see if introducing Kv4.2 could rescue the developmental NMDAR subunit deficits (Fig. 2). In adult Kv4.2-KO neurons, in response to acutely increasing Kv4.2 levels, ISF was reduced nearly threefold (Kv4.2-KO+Kv4.2g, 0.13 ± 0.3, $n = 7$; Fig. 2*A*,*B*) compared with uninfected adult Kv4.2-KO neurons (0.35 ± 0.05, $n = 10$; $p < 0.01$). Together, these results show that Kv4.2 expression is able to drive synaptic maturation in neonatal WT neurons and rescue the altered NMDAR subunit ratio in Kv4.2-KO neurons.

Expression of dominant-negative mutant of Kv4.2 (Kv4.2g^{W362F}) in CA1 neurons of organotypic slices have been previously shown to significantly reduce A-current levels and impact dendritic excitability (J. Kim et al., 2005). Here too we found that *in vivo* injection of Kv4.2g^{W362F} decreased A-current density (101.06 ± 7.16

pA/pF, $n = 6$) compared with uninfected neurons (127.20 ± 6.99, $n = 7$, $p < 0.05$) in whole-cell recordings. To determine whether acute downregulation of functional Kv4.2 alters GluN2A/2B expression levels in mature synapses, we injected virus containing Kv4.2g^{W362F} into adult WT hippocampus. Downregulating A-current function with Kv4.2g^{W362F} in adult WT mice caused an increase in synaptic ISF (WT, 0.11 ± 0.03, $n = 9$; WT+Kv4.2g^{W362F}, 0.31 ± 0.07, $n = 8$; $p < 0.05$; Fig. 2*C*,*D*), likely through an increase in GluN2B expression (Jung et al., 2008). These results, to our knowledge, provide the first experimental evidence that WT hippocampal neurons retain the ability to dynamically regulate GluN2 levels into adulthood. Bidirectional regulation of synaptic GluN2B/GluN2A levels in adult mice by Kv4.2 likely occurs through activity-dependent regulation of excitability by Kv4.2 channels, since Kv4.2g and its dominant-negative mutant (Kv4.2g^{W362F}) have opposing effects on synaptic development, despite differing by only a single amino acid.

Another synaptic change during development is the recruitment of AMPARs to previously silent synapses, which contain only NMDARs. In the hippocampus, these silent synapses progressively decrease during development as they are converted to functional synapses by synaptic activity (Kerchner and Nicoll, 2008). We used the minimal stimulation technique to estimate silent synapse prevalence in WT and Kv4.2-KOs by comparing the failure rates of EPSCs at −60 mV and +40 mV (Fig. 3). Stimulation intensity was adjusted such that ~50% of stimulations resulted in synaptic transmission failures at −60 mV, a voltage where primarily AMPAR-mediated EPSCs are detected given that NMDARs experience Mg^{2+}-block at this voltage. After 50 consecutive trials, the membrane potential was depolarized to +40 mV to relieve the Mg^{2+}-block of NMDARs and measure a mixed AMPAR- and NMDAR-mediated response. Thus, the fraction of silent synapses was considered to be the neurotransmission failure rate at −60 mV relative to the failure rate at +40 mV. Failure rate at +40 mV was significantly decreased compared to that at −60 mV in both neonatal WT (−60 mV, 0.61 ± 0.03; +40 mV, 0.34 ± 0.04, $n = 10$; $p < 0.01$; Fig. 3*B*) and Kv4.2-KO mice (−60 mV, 0.58 ± 0.05; +40 mV, 0.25 ± 0.02, $n = 6$, $p < 0.01$; Fig. 3*C*). Remarkably, while there was no difference in failure rate at −60 mV and +40 mV in adult WT mouse recordings (−60 mV, 0.52 ± 0.05; +40 mV, 0.49 ± 0.05, $n = 6$, $p > 0.05$; Fig. 3*D*), the failure rate of adult Kv4.2-KO recordings at +40 mV was significantly lower than the failure rate at −60 mV (−60 mV, 0.50 ± 0.04; +40 mV, 0.22 ± 0.04, $n = 6$, $p < 0.01$; Fig. 3*E*), indicating that there was a significant proportion of silent synapses remaining in adult Kv4.2-KO neurons.

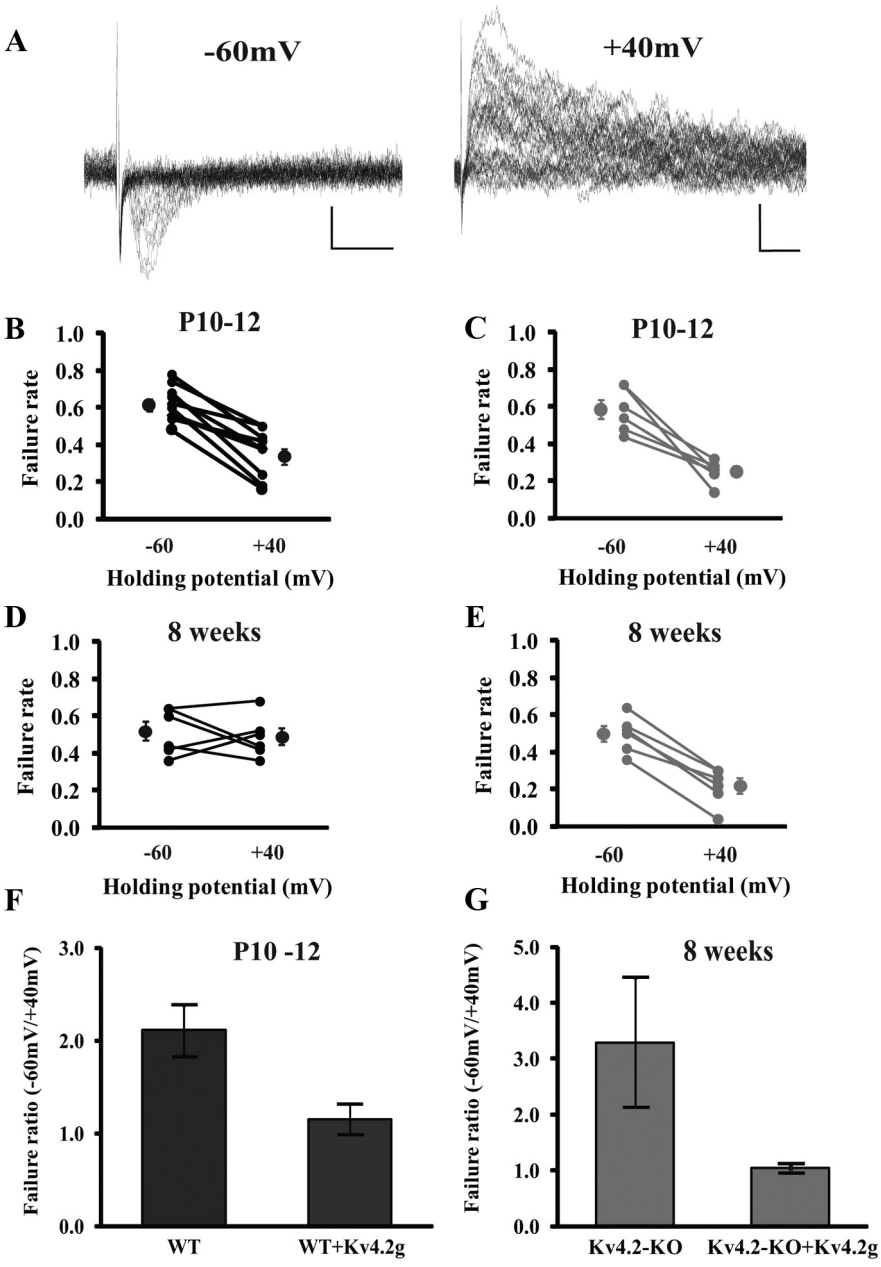

Figure 3. Increased silent synapse prevalence in adult Kv4.2-KO mice. ***A***, Example traces from a minimal stimulation experiment. Traces show 50 consecutive synaptic responses recorded at −60 mV and +40 mV holding potentials. Scale bars: left: 10 pA, 10 ms; right: 20 pA, 20 ms. ***B–E***, Synaptic failure rate at holding potentials of −60 mV and +40 mV for neurons from neonatal WT (***B***), neonatal Kv4.2-KO (***C***), adult WT (***D***), and Kv4.2-KO (***E***) mice. ***F***, ***G***, Decreased failure ratio (−60 mV/+40 mV) in Kv4.2g-infected neurons in both neonatal WT (***F***) and adult Kv4.2-KO (***G***) mice.

To see if reducing excitability by increasing A-currents could impact silent synapse fraction during development, we injected Kv4.2g into neonatal WT hippocampus. The results showed decreased failure ratio (failure rate at −60 mV/failure rate at +40 mV) in Kv4.2g-expressing neurons compared with uninfected WT neurons (neonatal WT+Kv4.2g, 1.15 ± 0.16, $n = 8$; neonatal WT, 2.12 ± 0.26, $n = 10$; $p < 0.01$; Fig. 3*F*). In addition, introducing Kv4.2g into adult Kv4.2-KO mice also resulted in a decreased failure ratio (adult KO+Kv4.2g, 1.05 ± 0.04, $n = 3$; adult KO, 3.29 ± 1.16, $n = 6$, $p < 0.05$; Fig. 3*G*). These findings show that decreasing excitability through Kv4.2g expression decreases the incidence of silent synapses, again strongly implicating Kv4.2 in synaptic maturation.

Discussion

Here we show that the activity level of subthreshold activating, A-type, voltage-gated K^+ channels can bidirectionally reorganize synaptic NMDAR subunit composition during development and into adulthood. Recordings from adult Kv4.2-KO mice suggested delayed synaptic maturation, showing a larger GluN2B/GluN2A NMDAR subunit ratio and increased silent synapse prevalence compared with adult WT hippocampal CA1 pyramidal neurons. Dynamic regulation of synaptic maturation state reported here is likely activity-dependent, as opposing results were found for Kv4.2 and its dominant-negative mutant, which differ only by a single amino acid in the pore of the channel. While it has been widely shown that synaptic activity influences synaptic development and glutamate receptor expression, and activity-dependent NMDAR subunit modification has been previously reported only in developing hippocampal neurons (Bellone and Nicoll, 2007; Kerchner and Nicoll, 2008), our findings show that activity-dependent synaptic NMDAR subunit remodeling can continue into adulthood. In a broad view, this might indicate a rejuvenation of mature synapses, allowing the neuron to overwrite existing stored information.

Another important finding presented here is that an abnormally large fraction of synapses onto CA1 neurons in adult Kv4.2-KO mice are functionally silent, containing NMDARs but not AMPARs. These synapses are normally found during the first postnatal week but then are gradually lost after the second postnatal week by activity-dependent insertion of AMPARs (Kerchner and Nicoll, 2008). Since hippocampal neurons from Kv4.2-KO mice exhibit increased intrinsic excitability and low threshold for LTP induction (Chen et al., 2006), enhanced activity-dependent AMPAR insertion might be expected. On the contrary, we found increased silent synapse expression in adult Kv4.2-KO mice, indicating that developmental AMPAR insertion was delayed in Kv4.2-KOs. Acute expression of Kv4.2 into the hippocampus of Kv4.2-KO mice reversed these abnormalities within 24 h of virus injection. Acute expression of Kv4.2 also accelerated synaptic maturation in neonatal WT mice. These findings may be explained by recent studies showing that GluN2B-containing NMDARs act to prevent AMPAR insertion into immature spines until appropriate synaptic activity triggers signals for their recruitment. Overexpression of GluN2B subunits in hippocampal neuronal cultures resulted in decreased surface expression of the AMPAR subunit, GluR1, while blocking GluN2B with ifenprodil increased the surface level of GluR1 (M. J. Kim et al., 2005). In addition, downregulation of GluN2B subunits using siRNA or early expression of GluN2A subunits in developing hippocampal CA1 pyramidal neurons resulted in decreased AMPAR-mediated mEPSCs frequency, suggesting GluN2B expression controls the number of functional synapses by regulating AMPAR insertion (Gambrill and Barria, 2011).

Increased silent synapse prevelance in Kv4.2-KO mice may therefore be a secondary effect of enhanced synaptic GluN2B expression through Kv4.2 regulation of CaMKII activation (Jung et al., 2008). Recently, Wang et al. (2011) showed that GluN2B subunits suppress synaptic AMPAR incorporation by negatively regulating local protein translation in dendrites and directly interacting with activated CaMKII. Although it has been widely known that CaMKII has a critical role in LTP expression by enhancing AMPAR function and expression, LTP at neonatal hippocampal synapses requires cAMP-dependent protein kinase A, not CaMKII (Yasuda et al., 2003), suggesting CaMKII may have a different role in AMPAR regulation in developing synapses. These results suggest that a role of GluN2B subunits during development is to maintain appropriate level of AMPARs by regulating protein synthesis in dendrites. In this regard, increased GluN2B fraction in Kv4.2-KO mice via enhanced CaMKII activity (Jung et al., 2008) appears to prevent AMPAR insertion, delaying synaptic maturation and perhaps contributing to their memory deficits (Lugo et al., 2012).

A recent study reported, in a mouse model of fragile X syndrome (Fmr1-KO mice), an altered developmental profile of NMDAR subtypes and the persistent presence of silent synapses in later developmental stages, indicating delayed synaptic maturation (Harlow et al., 2010). The *fmr1* gene produces fragile X mental retardation protein, which regulates neuronal development and synaptic plasticity by regulating mRNAs that are translated into numerous important synaptic molecules, such as PSD-95 and CaMKII (Bassell and Warren, 2008). Thus, loss of the *fmr1* gene results in an increase in abnormal dendritic spines (hyperabundance with a long, thin immature morphology), altered synaptic plasticity, and cognitive and behavioral deficits (Zhang et al., 2009; Krueger et al., 2011). Similar to Fmr1-KO mice, Kv4.2-KO mice display altered synaptic plasticity, intrinsic excitability, and deficits in learning and memory (Chen et al., 2006; Nerbonne et al., 2008). Since both Fmr1-KO and Kv4.2-KO mice exhibit functional control over synaptic activity, one can speculate that they might share overlapping mechanisms underlying synaptic modification and maturation. In fact, recent studies have suggested Fmr-1 protein control of Kv4.2 activity (Gross et al., 2011; Lee et al., 2011).

Developing brains are capable of robust activity-dependent synaptic plasticity while the capacity to induce synaptic plasticity declines with aging. These developmental changes in synaptic plasticity are accompanied by age-dependent cognitive function impairment (Barnes, 2003). Since NMDARs have important roles in synaptic plasticity and learning and memory, it is not surprising that alterations in NMDAR function and expression are found in aged rat hippocampus. In particular, knock-down of GluN2B subunits in young animals mimicked age-related cognitive decline as well as impaired LTP induction (Clayton et al., 2002). Conversely, overexpression of GluN2B leads to enhanced spatial memory performance and LTP (Tang et al., 1999). Our findings place A-type K^+ currents as integral contributors to a synaptic NMDAR signaling complex controlling age-dependent cognitive function.

References

Barnes CA (2003) Long-term potentiation and the ageing brain. Philos Trans R Soc Lond B Biol Sci 358:765–772. CrossRef Medline

Bassell GJ, Warren ST (2008) Fragile X syndrome: loss of local mRNA regulation alters synaptic development and function. Neuron 60:201–214. CrossRef Medline

Bellone C, Nicoll RA (2007) Rapid bidirectional switching of synaptic NMDA receptors. Neuron 55:779–785. CrossRef Medline

Birnbaum SG, Varga AW, Yuan LL, Anderson AE, Sweatt JD, Schrader LA (2004) Structure and function of Kv4-family transient potassium channels. Physiol Rev 84:803–833. CrossRef Medline

Bliss TV, Collingridge GL (1993) A synaptic model of memory: long-term potentiation in the hippocampus. Nature 361:31–39. CrossRef Medline

Chen X, Yuan LL, Zhao C, Birnbaum SG, Frick A, Jung WE, Schwarz TL, Sweatt JD, Johnston D (2006) Deletion of Kv4.2 gene eliminates dendritic A-type K+ current and enhances induction of long-term potentiation in hippocampal CA1 pyramidal neurons. J Neurosci 26:12143–12151. CrossRef Medline

Clayton DA, Mesches MH, Alvarez E, Bickford PC, Browning MD (2002) A hippocampal NR2B deficit can mimic age-related changes in long-term potentiation and spatial learning in the Fischer 344 rat. J Neurosci 22:3628–3637. Medline

Gambrill AC, Barria A (2011) NMDA receptor subunit composition con-

trols synaptogenesis and synapse stabilization. Proc Natl Acad Sci U S A 108:5855–5860. CrossRef Medline

Gaspar PA, Bustamante ML, Rojo LE, Martinez A (2012) From glutamatergic dysfunction to cognitive impairment: boundaries in the therapeutic of the schizophrenia. Curr Pharm Biotechnol 13:1543–1548. Medline

Gross C, Yao X, Pong DL, Jeromin A, Bassell GJ (2011) Fragile X mental retardation protein regulates protein expression and mRNA translation of the potassium channel Kv4.2. J Neurosci 31:5693–5698. CrossRef Medline

Harlow EG, Till SM, Russell TA, Wijetunge LS, Kind P, Contractor A (2010) Critical period plasticity is disrupted in the barrel cortex of FMR1 knockout mice. Neuron 65:385–398. CrossRef Medline

Jung SC, Kim J, Hoffman DA (2008) Rapid, bidirectional remodeling of synaptic NMDA receptor subunit composition by A-type K+ channel activity in hippocampal CA1 pyramidal neurons. Neuron 60:657–671. CrossRef Medline

Kerchner GA, Nicoll RA (2008) Silent synapses and the emergence of a postsynaptic mechanism for LTP. Nat Rev Neurosci 9:813–825. CrossRef Medline

Kim J, Wei DS, Hoffman DA (2005) Kv4 potassium channel subunits control action potential repolarization and frequency-dependent broadening in rat hippocampal CA1 pyramidal neurones. J Physiol 569:41–57. CrossRef Medline

Kim MJ, Dunah AW, Wang YT, Sheng M (2005) Differential roles of NR2A- and NR2B-containing NMDA receptors in Ras-ERK signaling and AMPA receptor trafficking. Neuron 46:745–760. CrossRef Medline

Krueger DD, Osterweil EK, Chen SP, Tye LD, Bear MF (2011) Cognitive dysfunction and prefrontal synaptic abnormalities in a mouse model of fragile X syndrome. Proc Natl Acad Sci U S A 108:2587–2592. CrossRef Medline

Lauver A, Yuan LL, Jeromin A, Nadin BM, Rodríguez JJ, Davies HA, Stewart MG, Wu GY, Pfaffinger PJ (2006) Manipulating Kv4.2 identifies a specific component of hippocampal pyramidal neuron A-current that depends upon Kv4.2 expression. J Neurochem 99:1207–1223. CrossRef Medline

Lee HY, Ge WP, Huang W, He Y, Wang GX, Rowson-Baldwin A, Smith SJ, Jan YN, Jan LY (2011) Bidirectional regulation of dendritic voltage-gated potassium channels by the fragile X mental retardation protein. Neuron 72:630–642. CrossRef Medline

Lugo JN, Brewster AL, Spencer CM, Anderson AE (2012) Kv4.2 knockout mice have hippocampal-dependent learning and memory deficits. Learn Mem 19:182–189. CrossRef Medline

Lynch MA (2004) Long-term potentiation and memory. Physiol Rev 84:87–136. CrossRef Medline

Malenka RC, Nicoll RA (1999) Long-term potentiation: a decade of progress? Science 285:1870–1874. CrossRef Medline

Nerbonne JM, Gerber BR, Norris A, Burkhalter A (2008) Electrical remodelling maintains firing properties in cortical pyramidal neurons lacking KCND2-encoded A-type K+ currents. J Physiol 586:1565–1579. CrossRef Medline

Sans N, Petralia RS, Wang YX, Blahos J 2nd, Hell JW, Wenthold RJ (2000) A developmental change in NMDA receptor-associated proteins at hippocampal synapses. J Neurosci 20:1260–1271. Medline

Tang YP, Shimizu E, Dube GR, Rampon C, Kerchner GA, Zhuo M, Liu G, Tsien JZ (1999) Genetic enhancement of learning and memory in mice. Nature 401:63–69. CrossRef Medline

Wallace TL, Ballard TM, Pouzet B, Riedel WJ, Wettstein JG (2011) Drug targets for cognitive enhancement in neuropsychiatric disorders. Pharmacol Biochem Behav 99:130–145. CrossRef Medline

Wang CC, Held RG, Chang SC, Yang L, Delpire E, Ghosh A, Hall BJ (2011) A critical role for GluN2B-containing NMDA receptors in cortical development and function. Neuron 72:789–805. CrossRef Medline

Yashiro K, Philpot BD (2008) Regulation of NMDA receptor subunit expression and its implications for LTD, LTP, and metaplasticity. Neuropharmacology 55:1081–1094. CrossRef Medline

Yasuda H, Barth AL, Stellwagen D, Malenka RC (2003) A developmental switch in the signaling cascades for LTP induction. Nat Neurosci 6:15–16. CrossRef Medline

Zhang J, Hou L, Klann E, Nelson DL (2009) Altered hippocampal synaptic plasticity in the FMR1 gene family knockout mouse models. J Neurophysiol 101:2572–2580. Medline

Zhao C, Wang L, Netoff T, Yuan LL (2011) Dendritic mechanisms controlling the threshold and timing requirement of synaptic plasticity. Hippocampus 21:288–297. CrossRef Medline